

Spin-Peierls vs Peierls distortions in a family of conjugated polymers

M. A. Garcia-Bach

Departament de Física Fonamental, Facultat de Física, Universitat de Barcelona, Diagonal 647, E-08028 Barcelona, Catalunya, Spain

R. Valenti

Institut für Physik, Universität Dortmund, 44221 Dortmund, Germany

D. J. Klein

Texas A & M University at Galveston, Galveston, Texas 77553-1675

(Received 16 December 1996; revised manuscript received 3 April 1997)

Distortions in a family of conjugated polymers are studied using two complementary approaches: within a many-body valence bond approach using a transfer-matrix technique to treat the Heisenberg model of the systems, and also in terms of the tight-binding band-theoretic model with interactions limited to nearest neighbors. The computations indicate that both methods predict the presence or absence of the same distortions in most of the polymers studied. [S0163-1829(97)08228-3]

I. INTRODUCTION

The recent discovery of the first inorganic spin-Peierls material, CuGeO_3 ,¹ has engendered a renewed interest in spin-Peierls systems, i.e., systems which present a structural distortion below the spin-Peierls temperature due to residual magnetoelastic couplings stabilizing the ground state, in analogy to Peierls distortion² associated with an electron-soft-phonon instability opening a band gap at the Fermi level. Recent experiments³ suggest that this is not an isolated case, and the pronounced decrease of susceptibility observed⁴ in α' - NaV_2O_5 is also due to a spin-Peierls transition.

The spin-Peierls transition was first observed in predominantly organic compounds as TTF-CuBDT ,⁵ TTF-TCNQ ,⁶ $(\text{TMTSF})_2\text{PF}_6$,⁷ or TTF-AuBDT .⁸ Theoretically, it has been studied (see for instance Refs. 9–14, and references therein) as a geometrical symmetry breaking for the lowest eigenstate of a Heisenberg Hamiltonian. Peierls and spin-Peierls phenomena are still a subject of discussion for many other polymers, since if a deviation occurs that lowers the chain's symmetry, then different symmetry-equivalent distorted ground states may arise which correspond to different thermodynamic phases and, at sufficiently low temperature, the possibility of solitonic excitations and/or conduction could arise.¹⁵

Furthermore, it has been argued¹⁶ that under similar structural circumstances a Peierls distortion is predicted for the simple Hückel tight-binding model of π -network strips if and only if a spin-Peierls distortion is also predicted from valence bond (VB) theory (or the formally equivalent $s = \frac{1}{2}$ Heisenberg model) at the simple resonance theoretic level. At this level of approximation the VB wave functions are restricted to equally weighted superpositions of special covalent VB singlet states, i.e., of Kekulé structures,¹⁷ where every π electron is coupled to a singlet state with one of their nearest neighbors. These Kekulé structures may be partitioned into long-range-ordered spin-pairing phases, the lowest-lying phase corresponding to the highest count of

Kekulé structures contributing to it. Within this approach, a spin-Peierls distortion is predicted if there are two maximum-cardinality-degenerate Kekulé phases (see Ref. 18, and references therein). Then this correspondence between Peierls and spin-Peierls instabilities implies that a zero-width band gap for a π -network polymer is predicted if and only if there are two such cardinality-degenerate Kekulé phases. The question then arises as to whether this correspondence is maintained when going beyond the resonance theoretic approximation.

For instance, the dimerization in polyacetylene has traditionally been interpreted in terms of band theory^{19,20} as a Peierls distortion. Recently, however, this dimerization has

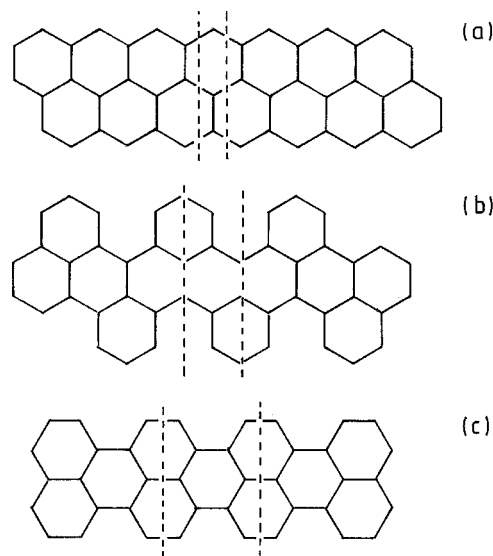


FIG. 1. Polymer systems. Fragments of (a) Polyacetylene (PAA), (b) poly(benz[m,n]anthracene) (PBA), and (c) polyperylene (PPR). The region between the vertical dashed lines defines the unit cell of PPR, while for PAA and PBA the reduced unit cell is instead identified.

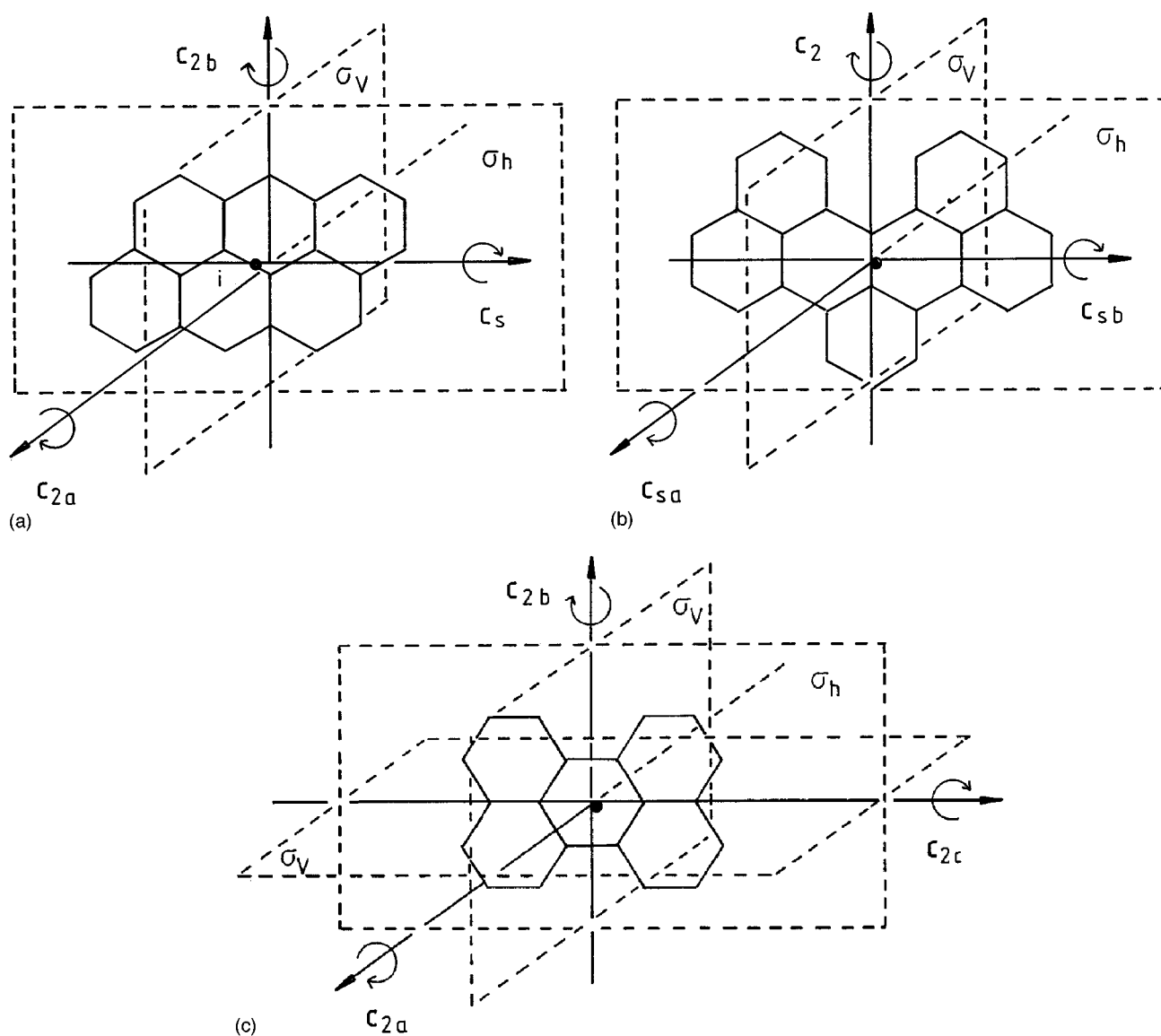


FIG. 2. Symmetry elements for (a) PAA, (b) PBA, and (c) PPR.

also been successfully explained²¹ with a Heisenberg-like Hamiltonian model²² as a spin-Peierls distortion, using both cluster-expanded wave functions and perturbation theory. This cluster-expanded many-body treatment of distortions has also been applied to the polyacene polymer,²³ which earlier has been extensively studied from the independent-particle point of view, since it exhibits an accidental zero-width band gap at a simple tight-binding level (see Refs. 23 and 24, and references therein), and a new quasidegeneracy has been predicted.

The comparison between the independent-particle and many-body VB treatments for degeneracy and symmetry breaking in polymers deserves further analysis. It is our purpose here to investigate the ground-state symmetries and degeneracies for several conjugated polymers using both a simple many-body VB framework and a simple tight-binding model. The rationale for these simplest models (with just nearest-neighbor interactions) is that they reveal distortive responses which qualitative dominate over the otherwise harmonic responses (e.g., associated with the σ electrons). That is, these simplest models should reveal dominant qualitative

features, which should persist independently of parameterization.

The polymers we focus our attention on are: polyacene (PAA), poly(benz[m,n]anthracene) (PBA), and polyperylene (PPR) (Fig. 1). All these systems exhibit a zero-width band gap at the simplest tight-binding level. So far, very few experimental results are available. Only PBA (Ref. 25) and PPR (Ref. 26) have already been synthesized. Theoretically PPR has been treated from the independent-particle point of view,^{27,28} and also using the valence effective Hamiltonian technique,²⁹ while as far as we know PBA has not been

TABLE I. Number of sites in the unit cell (uc) and in the reduced unit cell (ruc), and symmetry operations in the space group not including primitive translations.

Polymer	Sites in uc	Sites in ruc	Symmetries
PAA	6	3	$i, \sigma_h, C_{2a}, C_{2b}, \sigma_v, C_s$
PBA	14	7	$i, \sigma_h, C_2, C_{sa}, C_{sb}$
PPR	10		$i, \sigma_h, C_{2a}, C_{2b}, C_{2c}, \sigma_{v1}, \sigma_{v2}$

2 reduced unit cells

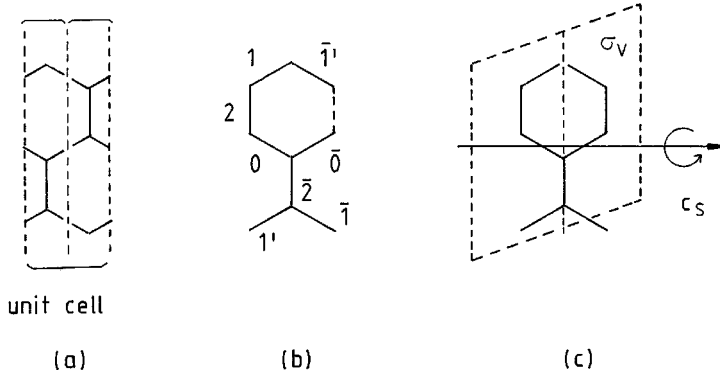


FIG. 3. PAA analysis. (a) Unit cell and reduced unit cell. (b) Labels associated with bonds. (c) Symmetry elements chosen to label distortions: the screw axis C_s and the vertical plane σ_v .

previously treated. PAA has been discussed in the literature, mostly from an independent-particle point of view,^{28,30–33} and less frequently from a resonance-theoretic approach,^{15,16} though it has not yet been synthesized. PAA can be seen, together with polyacetylene and polyacene, as the first members of a family of poly-trans-polyacetylenes, graphite being the final member of the family. All these can be thought of as special cases of ladder materials,³⁴ as already pointed out in Refs. 15, 32, and 33.

Within the many-body VB framework, we will consider the antiferromagnetically signed spin- $\frac{1}{2}$ Heisenberg model (for more general derivations of this model than those based on degenerate perturbation expansions see, for instance, Refs. 22 and 35, and references therein). Adequate many-body wave-function *Ansätze* provide variational upper bounds to the ground-state energy. Two different kinds of variational localized-site cluster expanded *Ansätze* have been considered: first a *resonating* VB (RVB) *Ansatz*, where the trial wave function is a weighted superposition over all singlets constructed as products of singlet pairs each involving two (not necessarily nearest-neighbor) sites at a time; and second a *Néel-state-based Ansatz*, where a Néel state is the zeroth-order wave function from which the trial wave-function is generated. We evaluate the matrix elements for each *Ansatz* with a transfer-matrix technique introduced previously.^{21,23,36–39} For the tight-binding band theory calculations we consider the so-called translationally adapted Hückel model limited to nearest neighbors.

This paper is organized as follows: in Sec. II the description of the polymers, their symmetries, and relevant distortions are given. In Sec. III we introduce briefly the translationally adapted Hückel model. In Sec. IV a description of the VB method is given in terms of the Heisenberg Hamil-

tonian, and trial wave functions are presented. Also, the technique to compute the physical magnitudes based on a transfer matrix is introduced and applied to obtain the ground-state energy of the systems. Results are presented and discussed in Sec. V. Finally, our conclusions can be found in Sec. VI.

II. DESCRIPTION OF THE POLYMERS AND THEIR SYMMETRIES

The systems studied are polymeric strips of finite width and infinite length ($L \rightarrow \infty$) (see Fig. 1). They are constructed with fused benzene rings, and can be seen as cut from the two-dimensional graphite or honeycomb lattice. Each site of the lattice is taken to represent an sp^2 -hybridized carbon atom with one π orbital perpendicular to the plane of the lattice and with one π electron per site. These strips are presumed to be *translationally symmetric* along L , with periodic boundary conditions, so that the strips may be divided into *unit cells* or eventually *reduced unit cells*, when the *space group* of the strip contains operations involving glide reflections. The *space group* of the strips include, along with the primitive translation, rotations C_n , reflections σ , and combination of rotations and reflections (improper rotations), coordinate inversion i , and screw rotations and glide reflections C_s , i.e., a combination of an improper twofold rotation or reflection with a nonprimitive translation of half a unit cell which by themselves do not leave the lattice invariant (see for instance Fig. 2 and Table I).

Of special interest are minimal subsets of symmetry operations, whose removal lead to (i) a band gap opening at the Fermi level, when analyzed from the band-theoretic point of view; and (ii) the lifting of the degeneracy of Kekulé phases,

2 reduced unit cells

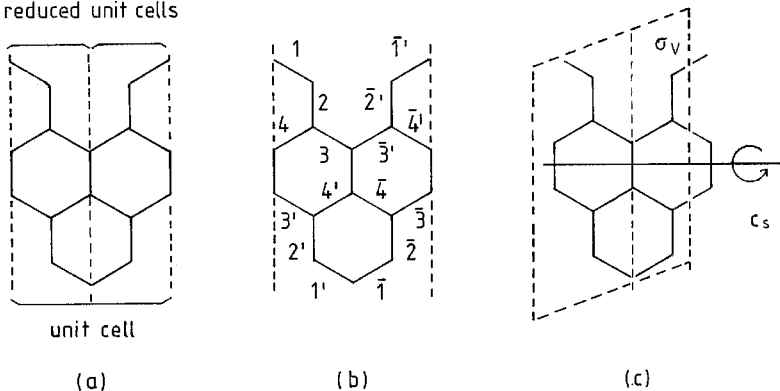


FIG. 4. PBA analysis. (a) Unit cell and reduced unit cell. (b) Bond labels. (c) Symmetry elements chosen to label distortions: a screw axis C_s and a vertical plane σ_v .

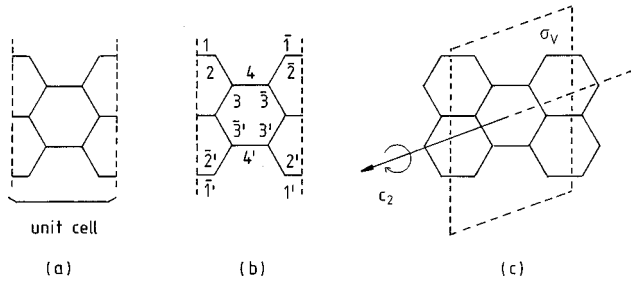


FIG. 5. PPR analysis. (a) Unit cell. (b) Bond labels. (c) Symmetry elements chosen to label distortions: a two-fold rotation axis C_2 perpendicular to the molecular plane, and a vertical plane σ_v .

if seen from the resonance-theoretic treatment. If a zero gap occurs at $k = \pi$ (as is frequently the case for benzenoid polymers) then such a minimal subset will be so as to no more than double the size of a unit cell.

When a symmetry is broken, there is a distortion parameter Δ_l associated to the stretching or shortening of the bond l , with bonds numbered as in Figs. 3, 4, and 5. Two symmetry elements are chosen to label the interesting distortions for every polymer as shown in Tables II, III, and IV, where appropriate constraints on Δ_l , imposed by the different symmetry breakings, are also shown. The distortions are classified as to symmetric (+1) or antisymmetric (-1) with respect to these two selected symmetry elements.

The PAA polymer is formed by benzene rings sharing four consecutive edges with neighboring rings as shown in Fig. 1(a). It can also be seen as a trimer of nondimerized parallel all-trans polyacetylene chains. The six-site unit cell can be broken into two three-site reduced unit cells, defined as the region between dashed lines in Fig. 1(a). In the band picture, there is a half-filled band and, consequently, a *zero-width band gap* is predicted, regardless of distortions which preserve the glide-reflection symmetry. In the simplest VB picture, i.e., resonance theory, there are two maximum-cardinality degenerate Kekulé phases. For instance, defining M as the number of “double bonds” crossed by an oblique line (see Fig. 6), there are two Kekulé phases $M = \text{even}$ equivalent to two $M = \text{odd}$ which do not mix because of the cyclic boundary conditions of the strip and they are degenerate since they each contain essentially a single Kekulé structure. A distortion that could open the band gap at the

TABLE II. Distortions considered for the PAA strip. For B distortions we identify subcases B_1 for $\Delta_1 > 0$ and $\Delta_2 = 0$, and B_2 for $\Delta_1 = 0$ and $\Delta_2 > 0$. For C distortions we identify subcases C_1 for $\Delta_1 > 0$ and $\Delta_0 = 0$, C_2 for $\Delta_1 = 0$ and $\Delta_0 > 0$, and C_3 for $\Delta_1 > 0$ and $\Delta_0 < 0$.

Distortion	C_s	σ_v	Restrictions on Δ_l
A	+1	-1	$\Delta_0 = \Delta_{\bar{0}} = \Delta_2 = \Delta_{\bar{2}} = 0$ $\Delta_1 = \Delta_{\bar{1}} = -\Delta_{1'} = -\Delta_{\bar{1}'}$
B	-1	+1	$\Delta_0 = \Delta_{\bar{0}} = 0$ $\Delta_1 = -\Delta_{\bar{1}} = -\Delta_{1'} = \Delta_{\bar{1}'}$ $\Delta_2 = -\Delta_{\bar{2}}$
C	-1	-1	$\Delta_1 = -\Delta_{\bar{1}} = \Delta_{1'} = -\Delta_{\bar{1}'}$ $\Delta_2 = \Delta_{\bar{2}} = 0$ $\Delta_0 = -\Delta_{\bar{0}}$

Fermi level and lift the degeneracy of the Kekulé phases requires the destruction of the glide-reflection symmetry. The distortions to be considered are then those which are *antisymmetric* with respect to interchange of the two reduced unit cells in a new unit cell.

PBA is formed by a polyacene strip where added benzene rings have been, top and bottom, alternatively fused on [see Fig. 1(b)]. A reduced unit cell can be defined for this system between the dashed lines in Fig. 1(b), with two seven-site reduced unit cells per unit cell. It is a half-filled band system and, like PAA, a zero-width band gap is predicted. Resonance theory, following Ref. 16, predicts two maximum-cardinality degenerate Kekulé phases. As in the PAA polymer, the interesting distortions that could open the band gap and lift the degeneracy are those that are *antisymmetric* under operations which interchange the two types of reduced unit cells.

The PPR polymer is formed by fused benzene rings as drawn in Fig. 1(c). The unit cell containing ten sites is defined between the dashed lines in the graph, and there is no smaller reduced unit cell for this system. The space group is generated by the point group D_{2h} and the translation operations along the strip [see Table I and Fig. 2(c)]. Differently from the rest of the polymers here, there is no glide-reflection symmetry operation for PPR. Furthermore, it does not have an odd number of π electrons per reduced unit cell, so that it does not correspond to a half-filled band system. Nevertheless, there is an accidental degeneracy at the Hückel level of approximation, so that it has a zero-width band gap anyway (see Sec. III). Correspondingly, resonance theory predicts two maximum-cardinality degenerate Kekulé phases.¹⁶ A *totally symmetric* distortion will also be considered for this system (see Table IV).

III. TRANSLATIONALLY ADAPTED HÜCKEL MODEL

The Hückel model is the simplest tight-binding model:

$$H_{Huck} = \sum_{\langle ni, mj \rangle, \sigma} \beta_{ni, mj} (c_{ni\sigma}^+ c_{mj\sigma} + c_{mj\sigma}^+ c_{ni\sigma}). \quad (1)$$

$c_{ni\sigma}^+$ ($c_{ni\sigma}$) are the creation (annihilation) electron operators on site i of unit cell n with spin σ and $\beta_{ni, mj}$ is the “Hückel resonance integral” (or hopping integral) between sites i and j in unit cells n and m , respectively. $\langle ni, mj \rangle$ indicates that the sum is restricted to nearest neighbors. Considering the translational invariance symmetry of the system, we can define translationally symmetry adapted states

TABLE III. Distortions considered for the PBA strip. All possible Δ_i , $i = 1, 2, 3$, and 4, are assumed to be mutually independent. For A distortions we identify subcases: A_1 for $\Delta_1 > 0$ and $\Delta_2 = \Delta_3 = \Delta_4 = 0$, and A_2 for $\Delta_1 = \Delta_2 = 0$, $\Delta_3 > 0$, and $\Delta_4 < 0$. For C distortions we identify subcases C_1 for $\Delta_1 > 0$, and the rest equal to zero, and C_2 for $\Delta_1 = \Delta_2 = 0$, $\Delta_3 > 0$, and $\Delta_4 < 0$.

Distortion	C_s	σ_v	Restrictions on Δ_l
A	+1	-1	$\Delta_i = \Delta_{\bar{i}} = -\Delta_{i'} = -\Delta_{\bar{i}'}$
B	-1	+1	$\Delta_i = -\Delta_{\bar{i}} = -\Delta_{i'} = \Delta_{\bar{i}'}$
C	-1	-1	$\Delta_i = -\Delta_{\bar{i}} = \Delta_{i'} = -\Delta_{\bar{i}'}$

TABLE IV. Distortions considered for the PPR strip, where $j=1, 2$, and 3 and $i=1, 2, 3$, and 4 . For C distortions we identify subcases C_1 for $\Delta_1=\Delta_4=0$, $\Delta_2>0$ and $\Delta_3>0$, and C_2 for $\Delta_1=\Delta_4=0$, $\Delta_2<0$ and $\Delta_3>0$. For D distortions we identify subcase D_1 for $\Delta_1=\Delta_2=0$, $\Delta_3>0$ and $\Delta_4>0$.

Distortion	C_2	σ_v	Restrictions on Δ_l
A	+1	-1	$\Delta_j=\Delta_{\bar{j}}=-\Delta_{j'}=-\Delta_{\bar{j}'}$ $\Delta_4=\Delta_{4'}=0$
B	-1	+1	$\Delta_j=\Delta_{\bar{j}}=-\Delta_{j'}=\Delta_{\bar{j}'}$ $\Delta_4=\Delta_{4'}=0$
C	-1	-1	$\Delta_i=-\Delta_{\bar{i}}=\Delta_{i'}=-\Delta_{\bar{i}'}$
D	+1	+1	$\Delta_i=\Delta_{\bar{i}}=\Delta_{i'}=\Delta_{\bar{i}'}$

$$|j;k\rangle \equiv \frac{1}{\sqrt{L^{n=1}}} \sum e^{ikn} |n,j\rangle, \quad k = \frac{2\pi n_k}{L},$$

$$n_k = 0, 1, \dots, L-1. \quad (2)$$

The matrix elements of the Hamiltonian between these new states are

$$\langle j;k|H|i;k'\rangle = \delta_{kk'} \sum_{\langle ni,mj\rangle} e^{-ik(n-m)} \beta_{ni,mj}. \quad (3)$$

Diagonalizing the Hamiltonian matrix elements, the energy bands $\varepsilon(k)$ are finally obtained.

Symmetry breaking can be considered taking $\beta_{ni,mj}$ as

$$\beta_{ni,mj} = \beta(1 + \Delta_{ni,mj}), \quad (4)$$

where $\Delta_{ni,mj}$ ($|\Delta_{ni,mj}| \ll 1$) is the distortion parameter, as introduced in Sec. II, that measures the strength of the distortion between sites ni and mj .

IV. VALENCE BOND METHOD

Within the VB picture we attempt here to go beyond resonance theory when solving the Heisenberg Hamiltonian:

$$H_{\text{Heis}} = \sum_{\langle ni,mj\rangle} J_{ni,mj} \vec{S}_{ni} \vec{S}_{mj} \quad (5)$$

$J_{ni,mj}$ is the ‘‘exchange integral’’ between nearest-neighbor sites ni , and mj and \vec{S}_{ni} denotes the spin operator for one electron on site ni .

$$J_{ni,mj} = J(1 + \Delta_{ni,mj}), \quad (6)$$

with $\Delta_{ni,mj}$ being the distortion parameter associated with the bond between sites ni and mj when there is a symmetry breaking.

While solving the Hückel model is an easy task, solving the Heisenberg Hamiltonian is in general a nontrivial problem. In order to obtain, along with the appropriate approximate wave functions, good variational upper bounds to the ground-state energy of this model, $E(\Delta)$, for the polymer systems, we consider two different types of cluster-expanded *Ansätze* that depend on variational parameters, each of which describes the *local* features of the system. Since our polymers are bipartite systems with total spin zero, we have considered a *Néel-state-based Ansatz* and a *RVB Ansatz*. These

Ansätze were introduced in Ref. 23 and we shall make here a brief description of them. Related *Ansätze* have also been successfully considered by other authors^{40,41} when solving the $s = \frac{1}{2}$ Heisenberg Hamiltonian for the square lattice.

A. Néel-state-based Ansatz (NSBA)

The cluster expanded wave-function *Ansatz* in this section is based upon the Néel state as a zeroth-order wave-function,

$$|\Phi_N\rangle = \prod_i^{i \in A} \alpha(i) \prod_j^{j \in B} \beta(j), \quad (7)$$

where A and B denote the two sets of sites such that each member of one set is a nearest neighbor solely to (some) sites of the other set, and $\alpha(i)$ [$\beta(i)$] indicate that the spin of the electron on site i is $+1/2$ ($-1/2$). A lowering of the energy, with respect to that of the Néel state, occurs for an *Ansatz* defined within a subspace spanned by $|\Phi_N\rangle$ and the states obtained when applying to $|\Phi_N\rangle$ the XY terms, $S_{ni}^{\pm} S_{mj}^{\mp}$, of the Heisenberg operator, an arbitrary number of times in an ‘‘unlinked’’ way. These additional states which are to be mixed with the Néel state can be generated in terms of the nearest-neighbor pair excitation operator

$$P \equiv \sum_{ni}^{\in A} \sum_{mj}^{\langle ni,mj\rangle} x_{ni,mj} S_{ni}^- S_{mj}^+, \quad (8)$$

where the $x_{ni,mj}$ are scalars to be optimized, and S_{ni}^+ and S_{ni}^- are spin raising and lowering operators on site ni

$$S_{ni}^{\pm} \equiv S_{ni}^x \pm i S_{ni}^y \quad (9)$$

From that, the Néel-state-based wave-function *Ansatz* (NSBA) will be a cluster-expansion in terms of P excitations acting on the Néel state,

$$|\Psi_N\rangle = U e^P |\Phi_N\rangle, \quad (10)$$

where U indicates that only unlinked terms are to be retained from the Taylor-series expansion. That is, $|\Psi_N\rangle$ is a wave-function where the Néel state is mixed with states that differ from it by an arbitrary number of couples of disjoint pairs of neighboring spins that have been flipped, each state in the

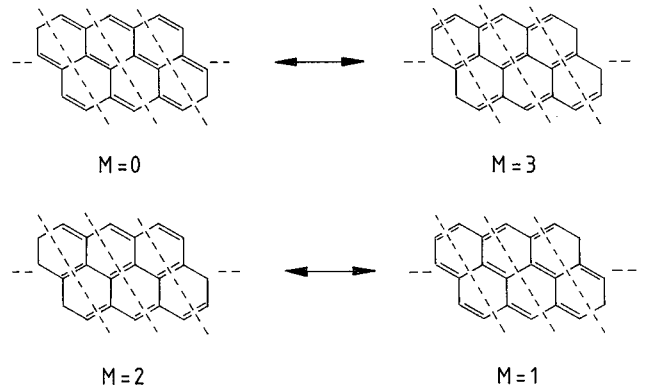


FIG. 6. Representation of the different nonmixing Kekulé phases of PAA, each one containing essentially one Kekulé structure.

superposition being weighted by the product of the variational parameters associated to the flips in that state.

B. Resonating valence bond *Ansätze*

In this approach we start with a one-bond-range RVB (1BR-RVB), that plays the fundamental zeroth-order role for the more elaborated three-bond-range RVB (3BR-RVB) *Ansatz* in the following.

1. One-bond-range RVB *Ansatz*

A 1BR-RVB $|\Psi_1\rangle$ is a weighted superposition of Kekulé states, i.e., nearest-neighbor VB states, where every site ni is spin paired to one of its neighbors mj . It can be written as

$$|\Psi_1\rangle = U_0 \prod_{ni} \sum_{mj} x_{ni,mj} (I - S_{ni}^- S_{mj}^+) |\Phi_N\rangle. \quad (11)$$

I is the identity operator, U_0 indicates that the terms to be retained are those where each site appears once and only once, and the weighting factor of a Kekulé state in Ψ_1 is a product of variational parameters $x_{ni,mj}$ associated with the singlet pairs ni, mj in the Kekulé state considered.

2. Three-bond-range RVB *Ansatz*

The 3BR-RVB is a weighted superposition of all the VB structures within a phase with each spin-pairing between A and B sublattice sites separated by no more than three bonds. In the usual form for cluster-expanded wave functions, it may be viewed as generated from the 1BR-RVB as follows: The XY terms, $S_{ni}^+ S_{mj}^-$, of the Heisenberg Hamiltonian acting on the 1BR-RVB wave function of Eq. (11) yield ‘‘long-bonded’’ states with pairings among three-bond distant neighbors, along with ‘‘neighbor-bonded’’ states already in Ψ_1 . These ‘‘long-bonded’’ states can be directly generated by the ‘‘recoupling’’ of two neighboring bond singlets in Ψ_1 (see Ref. 23). We may denote by \hat{q}_{ef} the operator related to such a recoupling between two bond singlets e and f . From $|\Psi_1\rangle$ we may build the 3BR-RVB allowing an arbitrary number of recouplings of two simply neighboring bond-singlets, i.e., unlinked pairs with one and only one site in a pair being a nearest neighbor to a site in the other pair. Then the overall 3BR-RVB excitation operator above the 1BR-RVB wave-function might be viewed to be

$$Q = \sum_{\langle e,f \rangle} x_{ef} \hat{q}_{ef}, \quad (12)$$

with x_{ef} being variational parameters, and where $\langle e,f \rangle$ indicates that the sum is restricted to simply neighboring bond-singlets. The corresponding *Ansatz* would then be

$$|\Psi_3\rangle = U e^Q |\Psi_1\rangle, \quad (13)$$

where again U indicates that only unlinked terms are to be retained. That is, in the Taylor-series expansion of e^Q one retains only products of \hat{q}_{ef} such that no pair index (e or f) shares any vertices with another pair index in the product. And Q and Ψ_1 are to be optimized simultaneously.

C. Expectation-value calculations by the transfer-matrix technique

The ground-state energy

$$E(\Psi) = \frac{\langle \Psi | H | \Psi \rangle}{\langle \Psi | \Psi \rangle} \quad (14)$$

is computed as a function of variational parameters for each of the above-introduced *Ansätze* assuming translational symmetry and cyclic boundary conditions along L . The way our *Ansätze* are chosen allows us to deal with the systems locally, so that one can define a transfer matrix²³ that describes the local features and reduces the computation of Eq. (14) to products of ‘‘small’’ matrices.^{21,23,36–39,42} Let us suppose there are imaginary vertical lines cutting the strip on translationally equivalent positions (including improper translations). We can define the *Ansatz*-dependent ‘‘local states’’ according to every possible local spin-pairing–spin-flip pattern around a given position determined by one of the imaginary vertical lines, and ultimately use this to compute $\langle \Psi | \Psi \rangle$. Thus these local states contain the contributions from both the *bra* and the *ket*. From the assumed translational symmetry, local states in every position are to be the same. Now, labeling these local states by e_t and t ranging over the whole set of local states, we let the transfer-matrix element

$$T_{ts} \equiv (e_t | T | e_s) \quad (15)$$

denote a weighted sum over the various ways a local state e_s may succeed a local state e_t . The weight of every contribution is obtained by considering the variational parameters associated to the way e_t evolves to e_s , and, eventually, additional factors coming from Pauling’s superposition rules.⁴³ The overlap is then evaluated in terms of the T matrix:

$$\langle \Psi | \Psi \rangle = \text{tr} T^L. \quad (16)$$

For $L \rightarrow \infty$, the largest eigenvalue Λ of T dominates, and the overlap reduces to

$$\langle \Psi | \Psi \rangle \approx \Lambda^L. \quad (17)$$

The Hamiltonian expectation value over $|\Psi\rangle$ can be obtained in a similar way introducing a ‘‘connection’’ matrix C , defined according to

$$\langle \Psi | H | \Psi \rangle = JL \langle \Psi | \sum_{\langle ni, mj \rangle} \overset{\text{per cell}}{\tilde{S}_{ni} \tilde{S}_{mj}} | \Psi \rangle = JL \text{tr} \{ T^{L-c} C \}, \quad (18)$$

where c measures the range of the interaction within the *Ansatz*. In our case, $c=2$, and the matrix element

$$C_{ts} = (e_t | C | e_s) \quad (19)$$

is a weighted sum over the various ways a local state e_s may succeed a local state e_t after c transfer-matrix-steps when the Hamiltonian operators per unit cell are present. In the long-length limit, Eq. (14) reduces to

$$E = \frac{1}{\Lambda^2} \frac{(\Lambda, l | C | \Lambda, r)}{(\Lambda, l | \Lambda, r)}, \quad (20)$$

TABLE V. Ground-state Heisenberg energy per site in J units for the family of π -network polymers studied. PA stands for polyacetylene. The first row corresponds to the energy obtained with a single Kekulé structure $|K\rangle$. $|\Psi_1\rangle$ stands for the 1BR-RVB *Ansatz* of Eq. (11), $|\Psi_3\rangle$ is the 3BR-RVB *Ansatz* of Eq. (13), $|\Phi_N\rangle$ is the Néel state, and $|\Psi_N\rangle$ the Néel-state-based *Ansatz* of Eq. (10). The last row corresponds to the exact ground-state energy which is known only for the 1D case.

E/JN	PA	PAA	PBA	PPR
$ K\rangle$	-0.37500	-0.37500	-0.37500	-0.37500
$ \Psi_1\rangle$	-0.37500	-0.37500	-0.4339(3)	-0.4435(2)
$ \Psi_3\rangle$	-0.41100	-0.4539(5)		
$ \Phi_N\rangle$	-0.25000	-0.333(3)	-0.3214(3)	-0.32500
$ \Psi_N\rangle$	-0.4279(1)	-0.4941(0)		-0.4906(2)
exact	-0.4431(5)			

where (Λ, l) and (Λ, r) are left and right eigenvectors corresponding to the maximum eigenvalue Λ of T . This expression is a function of the variational parameters associated with Ψ , and an upper bound to the exact ground-state energy is obtained. Implementation of a suitable numerical optimization yields the best upper bound. The energy expression (20) can be readily generalized when considering possible distortions. The connection matrix per unit cell can be understood as a sum of matrices $C_{ni,mj}$, each one concerning two-body interactions between neighboring sites ni and mj , weighted by the factor $1 + \Delta_{ni,mj}$ that modifies its interaction strength. Then

$$C = \frac{1}{2} \sum_i \sum_{mj}^{\in n} \langle ni, mj \rangle (1 + \Delta_{ni,mj}) C_{ni,mj}, \quad (21)$$

and the energy expectation evaluation is reduced to some ‘‘simple’’ matrix manipulations.

V. RESULTS AND DISCUSSION

Computations based on band theory at a Hückel tight-binding level of approximation (see Sec. III), and within VB theory with the cluster-expanded 1BR-RVB *Ansatz* and NSBA (see Sec. IV) were carried out for all polymer systems here described. For the PAA, the 3BR-RVB has also been used. In this case the 1BR-RVB *Ansatz* contains only one Kekulé structure, so it is especially appropriate to use the 3BR-RVB wave function and go beyond a single Kekulé-structure approximation. This circumstance differs from the rest of the polymers, where the number of Kekulé structures in the corresponding 1BR-RVB is large. The different VB upper bounds to the energy of the undistorted polymers are presented in Table V, together with that for polyacetylene. The lowest upper bound to the ground-state energy for the undistorted system is given by the NSBA.

A. PAA

The highest occupied Hückel tight-binding band and the lowest unoccupied band cross at $k = \pi$. Taking into account the perturbation $\Delta_{ni,mj}$ in the Hückel resonance integral, $\beta_{ni,mj} = \beta(1 + \Delta_{ni,mj})$, only the *totally antisymmetric* distor-

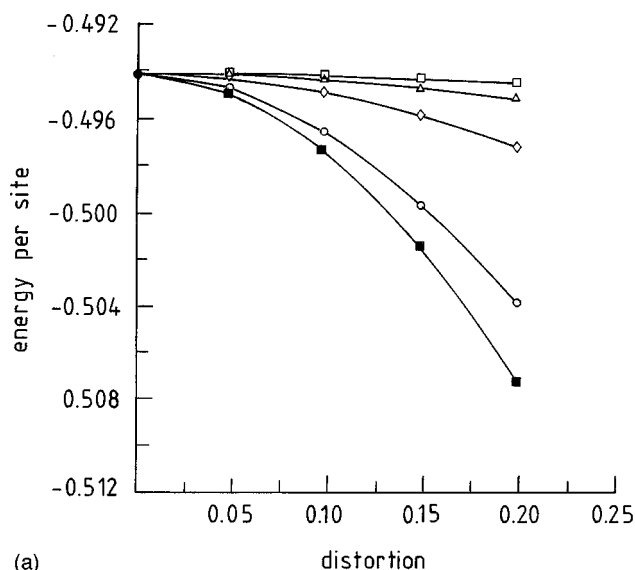
tion with respect to C_s and σ_v labeled as C_3 (see Table II) opens a gap at $k = \pi$. But the leading term of the energy lowering ΔE versus Δ is $\sim \Delta^2$, as it is the positive phonon energy contribution to be added. Thus band theory at this low level of approximation predicts neither the presence nor absence of a C_3 distortion for this system, the result depending on the final balance between these two contributions to the energy. Nevertheless, if interactions with more distant π centers are included, although small, linear terms in Δ are argued to arise,¹⁶ and then the distortion is favored.

Still, within band theory, this system has also been studied by other authors at different levels of approximation. Kertesz³¹ and Tanaka³² suggest a totally antisymmetric distortion, though leading to a quadratic small gap that could be suppressed by interchain interactions. The tight-binding self-consistent-field molecular-orbital method at the level of CNDO/2 (complete neglect of differential overlap) calculations suggests that the Peierls distortion does not take place so one can expect *metallic* behavior,³⁰ while Bozović²⁸ combining tight-binding calculations with group-theoretical arguments predicts distortions of type B (see Table II) as favored. Therefore, within band theory, predictions about the opening or not of a band gap at the Fermi level, or the distortion driving it, depend crucially on the level of approximation.

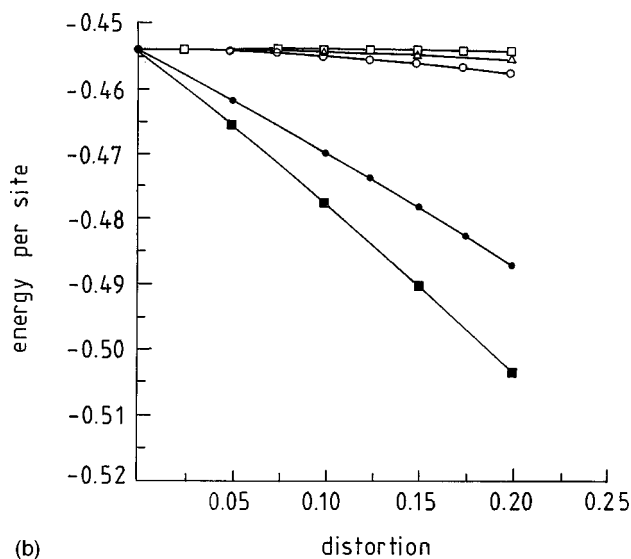
Let us consider now the many-body VB method. The ground state energy has been obtained using the NSBA and both the 1BR- and the 3BR-RVB *Ansätze* of Sec. IV, as a function of Δ for the different distortions A , B_1 , B_2 , C_1 , C_2 , and C_3 (see Table II). Transfer and connection matrices of dimensions 14×14 (for the NSBA) and 60×60 (for the 3BR-RVB *Ansatz*) were needed in order to carry out computations. The energy for the different distortions when the NSBA is used has been plotted as a function of Δ in Fig. 7(a), while results obtained with the 3BR-RVB *Ansatz* are presented in Fig. 7(b). Plots from the 1BR-RVB *Ansatz* are not given, since they are qualitatively identical to those from the 3BR-RVB ones. Comparing NSBA and RVB *Ansätze*, it can be seen that the ordering of ΔE for the different distortions is the same in any case, the strongest lowering corresponding to the C_3 distortion.

Nevertheless, while the energy response to A , B and C distortions is linear for the RVB *Ansätze*, clearly predicting a C_3 distorted ground-state, in the NSBA case they still go as $\sim \Delta^2$. Fitting the results in a parabolic curve, it is obtained that $\Delta E \sim -1.923\Delta^2$. Again a distortion is not clearly predicted with our NSBA. A comparison of the coefficients coming from this term and those from the phonon energy should be made in order to decide whether this *Ansatz* is able to predict or not to predict a C_3 distortion. This ambiguity of prediction in some sense rationalizes earlier contradictory results: via the numerical band theory of Yamabe *et al.*,³⁰ predicting an undistorted ground-state, and via band-group-theoretic considerations by Bozović,²⁸ predicting a B distortion.

Although the RVB ground-state energy is higher than the NSBA, its predictions on ground-state instabilities are based upon the known global-singlet character of the ground state along with its local-singlet character, leading to asymptotically orthogonal and noninteracting phases responding essentially independently to distortions. Relaxation of this local-singlet character would imply the inclusion of pairings



(a)



(b)

FIG. 7. Energy as a function of the distortion parameter Δ in PAA (a) when the Néel-state-based *Ansatz* $|\Psi_N\rangle$ is considered, (b) when the 3BR-RVB *Ansatz* $|\Psi_3\rangle$ is considered. The curves correspond to the different distortions given in Table II: (\square) B_1 , (\triangle) B_2 , (\diamond) C_2 , (\circ) A , (\bullet) C_1 , and (\blacksquare) C_3 .

between distant sites, leading to undesirable long-range correlations of the type in the Néel state. Then we expect a C_3 distorted ground state as predicted by RVB. Furthermore, NSBA at this lower level, with only two-site excitations, does not always seem sensitive to instabilities as at higher order, such as for polyacetylene;²¹ then we expect that the distortion could also be clearly predicted when going to a higher-order NSBA. Also, it can be argued that inclusion of slightly longer-range interactions (as between next-nearest neighbors) in the Hamiltonian will increase the “frustration” and the NSBA energy, whereas the RVB expectations will change but little. Thus there is a tendency to invert the energy ordering of these states. Still another argument favoring RVB predictions is that the NSBA is not a pure singlet, as the ground state is known to be. Also the RVB type *Ansatz* accords more closely to a classical organic chemical view of these polymers.

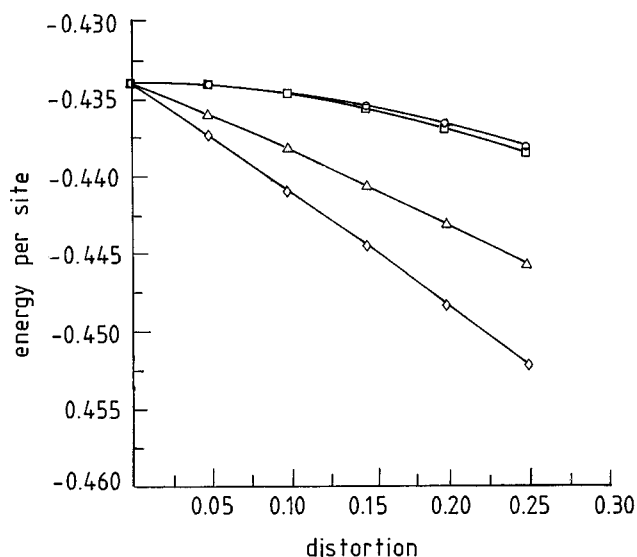


FIG. 8. Energy as a function of the distortion parameter Δ in PBA when the 1BR-RVB *Ansatz* $|\Psi_1\rangle$ is considered. The curves correspond to the different distortions given in Table III: (\circ) A_1 , (\square) A_2 , (\triangle) C_2 , and (\diamond) C_1 .

B. PBA

The lowest occupied Hückel tight-binding band and the highest unoccupied one cross at $k = \pi$, so it is a zero-width band-gap system. From all the possible distortions considered in Table III, only the *totally antisymmetric* distortions C_1 and C_2 open a gap with an energy dependence linear in Δ . Therefore, band theory predicts that the system will distort. In the VB picture the possible distortions in PBA have been studied with the 1BR-RVB *Ansatz*. For this system we only carried out calculations with this *Ansatz* for two reasons: (i) the 1BR-RVB *Ansatz* already gives a good upper bound to the ground-state energy because there is mixing of Kekulé states, and (ii) the dimension of the transfer and connection matrices for the 3BR-RVB and the Néel-state-based *Ansätze* grow substantially with respect to the 1BR-RVB one. In Fig. 8 the energy of the 1BR-RVB *Ansatz* is plotted as a function of Δ for the distortions A_1 , A_2 , C_1 , and C_2 classified in Table III. The most favored distortions are the *totally antisymmetric* ones C_1 and C_2 , in particular C_1 with a dependence $\sim \Delta$. This result agrees with the predictions given from band theory, concluding that complementary approaches lead to the same kind of distortions for this system.

C. PPR

PPR is not a half-filled band system but the Hückel model predicts an accidental zero-width band gap at $k=0$. A , B , C and D distortions (see Table IV) have been considered. The distortions C_1 and C_2 open a gap at $k=0$ weakly, with an energy dependence $\Delta E \sim \Delta^2$. But the *totally symmetric* distortion D_1 opens a band gap with an energy response linear in Δ . This result agrees with the predictions given by Bozović²⁸ and Tanaka *et al.*²⁷ In Fig. 9(a) the Néel-state-based energy obtained, using 5×5 transfer and connection matrices, is plotted as a function of Δ for various possible distortions (see Table IV). Clearly the *totally symmetric* distortion, D_1 is favored with a linear energy dependence on

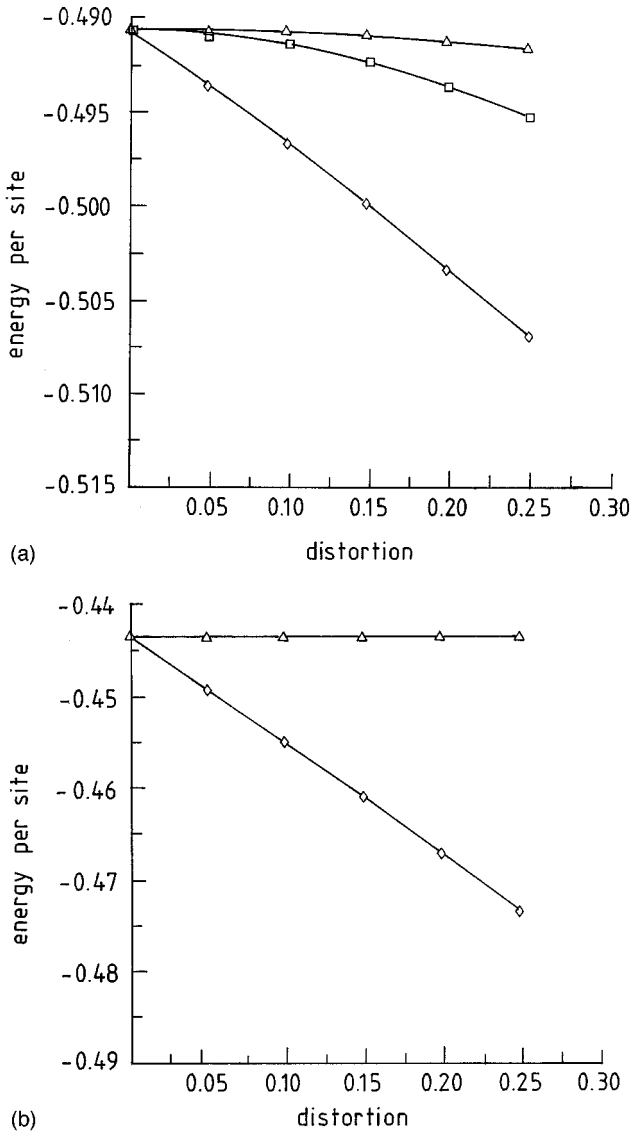


FIG. 9. Energy as a function of the distortion parameter Δ in PPR: (a) when the Néel-state-based *Ansatz* $|\Psi_N\rangle$ is considered; (b) when the 1BR-RVB *Ansatz* $|\Psi_1\rangle$ is considered. The curves correspond to the different distortions given in Table IV: (Δ) C_1 , (\square) C_2 , and (\diamond) D_1 .

Δ . Also in Fig. 9(b) the 1BR-RVB energy is plotted for the various distortions as a function of Δ and results agree with the NSBA energy, namely that the D_1 distortion is the most favored one with a linear dependence in Δ . As in PBA, the 1BR-RVB *Ansatz* already gives a good upper bound due to the mixing of Kekulé states.

Band theory and the many-body VB method predict the same distortional behavior for this system, i.e., the system is unstable to a *totally symmetric* D_1 distortion. Some evidence exists for polyperylene synthesis,²⁶ but further experimental information on the structure (and properties) of this system is still needed.

VI. CONCLUSIONS

We have presented, both with the simple Hückel tight-binding band theory and with a Heisenberg model Hamiltonian (or, equivalently, the VB model), a study of the

ground-state nature of a family of polymers: polyacene, poly(benz[m,n]anthracene), and polyperylene. We have focused our attention on correspondences between Peierls and spin-Peierls instabilities predictions, when analyzed from these two complementary approaches.

Upper bounds to the energy of the Heisenberg model in each case have been obtained with two alternative localized-site cluster-expanded wave functions, i.e., RVB-type *Ansätze* and a Néel-based *Ansatz*. We have shown that simple expressions of the physical magnitudes we were interested in were easily obtained by using the transfer-matrix technique of Ref. 23.

From our results, it is concluded that the RVB wave functions considered, which are restricted to 1BR type for all the systems other than PAA, do not give our best upper bound to the ground-state energy of the undistorted systems. Nevertheless, they are relevant for studying such phenomena as the *spin-Peierls instability* and elementary excitations such as hole excitations or excitonic excitations, as already pointed out.³⁸ Moreover the RVB *Ansätze* have a global-singlet character and a local-singlet character, precluding long-range order of the type of the Néel state, and generally improve relative to Néel-based *Ansätze* upon inclusion of higher-order (frustrative) terms in an elaborated Heisenberg model.

The Néel-state-based *Ansatz* gives a fairly good upper bound to the ground-state energy for all the systems considered. For the nearest-neighbor model considered, this *Ansatz* always yields lower energy than the RVB ones for undistorted systems. We have shown that, with such a simple Néel-state-based wave function, the corresponding energy is notably lower than the energy of the Néel state, while computations remain fairly simple. The Néel-state-based *Ansatz* predicts, for the polymers studied, the same distortions as the RVB description, except for the case of polyacene where this *Ansatz* in our current simple considerations does not show whether the distortion is going to take place or not, although the strongest lowering of the energy also correspond to a *totally antisymmetric* distortion.

From the Heisenberg Hamiltonian, or equivalently from the VB model, we have obtained the following:

(1) PAA shows a *totally antisymmetric* distortion from the RVB, while the NSBA is not conclusive, depending on the balance between electronic energy lowering and the phonon energy contribution.

(2) PBA shows a *totally antisymmetric* distortion.

(3) PPR is unstable to a *totally symmetric* distortion.

Within the band-theoretic picture, the Hückel tight-binding model has been studied for all the same polymers. Results obtained for our π -network system are as follows:

(1) PAA could show a *totally antisymmetric* distortion at a simple Hückel level, depending on the balance between electronic energy lowering and the phonon energy contribution. Other approximations already in the literature^{28,30} yield contradictory results.

(2) PBA shows a *totally antisymmetric* distortion.

(3) PPR shows a *totally symmetric* distortion.

Comparing band theory and the Heisenberg model results, it can be concluded that predictions of these two models based on opposite (or complementary) limits seem to lead to similar consequences under similar structural circumstances, i.e., both approaches predict the presence or absence of the

same instability to symmetry for the polymers. It is to be noted that the band-theoretic results depend crucially on the level of approximation, as it is observed in the study of polyacetylene, where this picture at different levels of approximation gives rise to different predictions. On the other hand, the Heisenberg model has proven to give predictions consistent from one level to another. Even in the case of PAA, where NSBA cannot make a clear prediction as it happens with band theory at its lower level, NSBA still shows the strongest lowering of the energy for the very same distortion suggested by RVB. Since the NSBA at this lower level, with only two-site excitations, does not always seem so sensitive to instabilities as at higher orders, such as happens with polyacetylene.²¹ That is, the distortion sometimes seems to only occur with a higher order NSBA, in agreement with RVB results. Therefore, it seems that the VB model, which includes correlation explicitly, gives a good description of these benzenoid systems, predicting spin-Peierls distortions whenever a Peierls distortion is also predicted. These results modify earlier suggestions (see Ref. 44) that inclusion of correlation *a posteriori*, as a perturbation, diminishes the distortion. That is, we find any diminishment does not go to zero in the (strong correlation) Heisenberg-model limit, and indeed the RVB results indicate a stronger response to distortions (at least at the undistorted point on the potential-energy hypersurface).

It has been shown that this treatment is computationally feasible especially for quasi-one-dimensional systems where the transfer-matrix technique proves to be a powerful tool of computation. It is important to note that the results are developed in terms of quantities which remain finite as the strip length goes to infinity. It is of some interest to compare the computational effort involved in the tight-binding approach versus that involved in our transfer-matrix cluster-expansion approach (for either RVB or Néel-state-based wave functions). The matrices $\mathbf{H}(k)$ of Eq. (3) and \mathbf{T} of Eq. (15) arise in these respective approaches and are both finite indepen-

dently of $L \rightarrow \infty$. Both types are to be diagonalized, but there are some differences:

(1) Typically \mathbf{T} increases in size much more rapidly with unit-cell “width” than does $\mathbf{H}(k)$ (though these behaviors are reversed if the unit-cell “length” is considered instead).

(2) The total energy requires sampling many of the $L \rightarrow \infty$ $\mathbf{H}(k)$ matrices (varying smoothly with wave vector k), whereas for given parameters there is but one \mathbf{T} matrix to treat.

(3) The optimal total energy for the cluster expansions entails treating \mathbf{T} matrices for numerous variational parameter values whereas there is not much repetition with the $\mathbf{H}(k)$.

Notably if one goes beyond the tight-binding method to Hartree-Fock (or density-functional) approaches this last noted difference no longer occurs. Evidently the computational effort via either SCF or our cluster expansion is roughly comparable (at least for linear polymers with modestly sized unit cells).

The analysis carried out in this paper would require experimental testing. Though the synthesis of some of the systems considered, like PAA, seems quite difficult to achieve, there are hopes in this direction. Finally, some aspects of this treatment are not restricted only to the model Hamiltonian and the ground-state *Ansätze* presented, but can be applied to any system with effective short-range interactions if described by a localized-site cluster expanded ground-state wave function.

ACKNOWLEDGMENTS

The authors acknowledge the University of Barcelona for computer facilities and CPU time. One of us (M.A.G.B.) acknowledges the DGICYT (Project No. PB95-0884). R.V. acknowledges support through the Deutsche Forschungsgemeinschaft. D.J.K. acknowledges support to the Welch Foundation of Houston (Texas).

-
- ¹ M. Hase, I. Terasaki, and K. Uchinokura, *Phys. Rev. Lett.* **70**, 3651 (1993).
- ² R. E. Peierls, *Quantum Theory of Solids* (Clarendon, Oxford, 1955).
- ³ M. Weiden, R. Hauptmann, C. Geibel, F. Steglich, M. Fischer, P. Lemmens, and G. Güntherodt, *Z. Phys. B* **103**, 1 (1997).
- ⁴ M. Isobe and Y. Ueda, *J. Phys. Soc. Jpn.* **65**, 1178 (1996).
- ⁵ J. W. Bray, H. R. Hart, Jr., L. V. Interrante, J. S. Jacobs, J. S. Kasper, G. D. Watkins, S. H. Wee, and J. C. Bonner, *Phys. Rev. Lett.* **35**, 744 (1975).
- ⁶ See, J. J. André, *Recent Advances in the Quantum Theory of Polymers*, Lecture Notes in Physics Vol. 113 (Springer-Verlag, Berlin, 1980).
- ⁷ K. Bechgaard, C. S. Jacobsen, K. Mostensen, H. J. Pedersen, and N. Thorup, *Solid State Commun.* **33**, 1119 (1980).
- ⁸ J. W. Bray *et al.*, in *Extended Linear Chain Compounds*, edited by J. S. Miller (Plenum, New York, 1985).
- ⁹ G. Beni and P. Pincus, *J. Chem. Phys.* **57**, 3531 (1972).
- ¹⁰ L. N. Bulaevskii, A. L. Buzdin, and D. I. Khomskii, *Solid State Commun.* **27**, 5 (1978).
- ¹¹ D. J. Klein and M. A. Garcia-Bach, *Phys. Rev. B* **19**, 877 (1979).
- ¹² M. C. Cross and D. S. Fisher, *Phys. Rev. B* **19**, 402 (1979); M.C. Cross, *ibid.* **20**, 4606 (1979).
- ¹³ J. Kondo, *Physica (Amsterdam)* **98B**, 176 (1980).
- ¹⁴ T. Nakano and H. Fukuyama, *J. Phys. Soc. Jpn.* **49**, 1679 (1980).
- ¹⁵ W. A. Seitz, D. J. Klein, T. G. Schmalz, and M. A. Garcia-Bach, *Chem. Phys. Lett.* **115**, 139 (1985).
- ¹⁶ D. J. Klein, T. G. Schmalz, W. A. Seitz, and G. E. Hite, *Int. J. Quantum Chem. Quantum Biol. Symp.* **19**, 707 (1986).
- ¹⁷ L. Pauling, *The Nature of Chemical Bond* (Cornell University Press, Ithaca, NY, 1958).
- ¹⁸ D. J. Klein, T. P. Zivković, and R. Valentí, *Phys. Rev. B* **43**, 723 (1991).
- ¹⁹ H. C. Longuet-Higgins and L. Salem, *Proc. R. Soc. London, Ser. A* **25**, 172 (1959).
- ²⁰ W.-P. Su, J. R. Schrieffer, and A. J. Heeger, *Phys. Rev. Lett.* **42**, 1698 (1979); *Phys. Rev. B* **22**, 2095 (1980).
- ²¹ M. A. Garcia-Bach, P. Blaise, and J.-P. Malrieu, *Phys. Rev. B* **46**, 15 645 (1992).
- ²² D. Maynaud, M. A. Garcia-Bach, and J.-P. Malrieu, *J. Phys. (France)* **47**, 207 (1986).

- ²³ M. A. Garcia-Bach, A. Peñaranda, and D. J. Klein, *Phys. Rev. B* **45**, 10 891 (1992).
- ²⁴ Y.-D. Gao and H. Hosoya, *Theor. Chim. Acta* **81**, 105 (1992).
- ²⁵ K. Tanaka, K. Ohzeki, and T. Yamabe, *Synth. Met.* **9**, 41 (1984).
- ²⁶ M. Murakami and S. Yoshimura, *Mol. Cryst. Liq. Cryst.* **118**, 95 (1985).
- ²⁷ K. Tanaka, K. Ueda, T. Koike, and T. Yamabe, *Solid State Commun.* **51**, 943 (1984).
- ²⁸ I. Bozović, *Phys. Rev. B* **32**, 8136 (1985).
- ²⁹ J. L. Bredas and R. H. Baughman, *J. Chem. Phys.* **83**, 1316 (1985).
- ³⁰ T. Yamabe, K. Tanaka, K. Ohzeki, and S. Yata, *Solid State Commun.* **44**, 823 (1982).
- ³¹ M. Kertesz and R. Hoffmann, *Solid State Commun.* **47**, 97 (1983).
- ³² K. Tanaka, S. Yamashita, H. Yamabe, and T. Yamabe, *Synth. Met.* **17**, 143 (1987).
- ³³ D. J. Klein, *Chem. Phys. Lett.* **217**, 261 (1994).
- ³⁴ E. Dagotto and T. M. Rice, *Science* **271**, 618 (1996).
- ³⁵ E. N. Economu and C. T. White, *Phys. Rev. Lett.* **38**, 289 (1977); E. N. Economu and P. Mihas, *J. Phys. C* **10**, 5017 (1977); R. D. Poshusta and D. J. Klein, *Phys. Rev. Lett.* **48**, 1555 (1982); R. D. Poshusta and D. J. Klein, *J. Mol. Struct.* **229**, 103 (1991).
- ³⁶ D. J. Klein, G. E. Hite, and T. G. Schmalz, *J. Comput. Chem.* **7**, 443 (1986).
- ³⁷ M. A. Garcia-Bach, D. J. Klein, R. Valentí, *Int. J. Mod. Phys. B* **1**, 1035 (1988); D. J. Klein, M. A. Garcia-Bach, and R. Valentí, *ibid.* **1**, 2159 (1989).
- ³⁸ D. J. Klein, M. A. Garcia-Bach, and W. A. Seitz, *J. Mol. Struct.* **185**, 275 (1989); M. A. Garcia-Bach, R. Valentí, and D. J. Klein, *ibid.* **185**, 287 (1989).
- ³⁹ M. A. Garcia-Bach, R. Valentí, S. A. Alexander, and D. J. Klein, *Croat. Chem. Acta* **64**, 415 (1991).
- ⁴⁰ S. Liang, B. Doucot, and P. W. Anderson, *Phys. Rev. Lett.* **61**, 365 (1988).
- ⁴¹ S. Sachdev, *Phys. Rev. B* **39**, 12 232 (1989).
- ⁴² M. Havelio, *Phys. Rev. B* **54**, 11 929 (1996).
- ⁴³ L. Pauling, *J. Chem. Phys.* **1**, 280 (1933).
- ⁴⁴ S. N. Dixit and S. Mazumdar, *Phys. Rev. B* **29**, 1824 (1984).